Structural Studies of N- and C-Terminally Truncated Human Apolipoprotein A-I†

Yiling Fang, Olga Gursky, and David Atkinson*

Department of Physiology and Biophysics, Boston University School of Medicine, 715 Albany Street, Boston, Massachusetts 02118

Received January 27, 2003; Revised Manuscript Received April 10, 2003

ABSTRACT: Apolipoprotein A-I (apoA-I) plays an important structural and functional role in lipid transport and metabolism. This work is focused on the central region of apoA-I (residues 60−183) that is predicted to contain exclusively amphipathic α-helices. Six N- and/or C-terminally truncated mutants, Δ(1−41), Δ(1−59), Δ(198−243), Δ(209−243), Δ(1−41,185−243), and Δ(1−59,185−243), were analyzed in their lipid-free state in solution at pH 4.7−7.8 by far- and near-UV CD spectroscopy. At pH 7.8, all mutants show well-defined secondary structures consisting of 40−52% α-helix. Comparison of the α-helix content in the wild type and mutants suggests that deletion of either the N- or C-terminal region induces helical unfolding elsewhere in the structure, indicating that the terminal regions are important for the integrity of the solution conformation of apoA-I. Near-UV CD spectra indicate significant tertiary and/or quaternary structural changes resulting from deletion of the N-terminal 41 residues. Reduction in pH from 7.8 to 4.7 leads to an increase in the mutant helical content by 5−20% and to a large increase in thermal unfolding cooperativity. Van't Hoff analysis of the mutants at pH 4.7 indicates melting temperatures T_m ranging from 51 to 59 °C and effective enthalpies $\Delta H_v(T_m) = 35 \pm 5$ kcal/mol, similar to the values for plasma apoA-I at pH 7.8 ($T_m = 57$ °C, $\Delta H_v = 32$ kcal/mol). Our results provide the first report of the pH effects on the secondary, tertiary, and/or quaternary structure of apoA-I variants and indicate the importance of the electrostatic interactions for the solution conformation of apoA-I.

Apolipoprotein A-I (apoA-I, 28 kDa, 243 amino acids), the major protein component of high-density lipoprotein (HDL),[1] was one of the first apolipoproteins to be identified and characterized and has been the subject of intense investigation because of its well-documented antiatherogenic properties. Reduced plasma levels of HDL and apoA-I are the hallmark of dyslipidemia, which is one of the key risk factors for atherosclerosis and cardiovascular disease (*1*). The antiatherogenic action of HDL and apoA-I is mediated mainly via their role in reverse cholesterol transport (*2*). ApoA-I stabilizes the HDL assembly, acts as the major activator for lecithin:cholesterol acyltransferase (LCAT) (*3*), serves as a ligand for the hepatic HDL receptor SR-BI (*4*), and promotes cholesterol efflux from cells. Thus, apoA-I is essential for the structure and antiatherogenic function of HDL.

ApoA-I adopts three distinct physiologically important conformations: lipid free, lipid poor, and lipid bound. A variety of models have been proposed for the structures of apoA-I in these different states. The structure and related function of lipid-free apoA-I in aqueous solution have been most extensively explored by many groups using mutagenesis techniques (reviewed in refs *5* and *6*).

The secondary structure of apoA-I, as well as other exchangeable apolipoproteins, is comprised of amphipathic α-helices (*7*). On the basis of circular dichroism (CD) spectroscopic studies and amino acid sequence analysis, apoA-I has been predicted to comprise a series of 22-mer and 11-mer sequence repeats forming amphipathic α-helices punctuated by prolines (*8*−*10*). The N-terminal region (residues 1−57), which contains the most ambiguously defined structure, is thought to be important in maintaining the lipid-free apoA-I conformation (*11*). The central domain (residues 60−183), which contains very well-defined clearly demarcated amphipathic α-helices, is important for LCAT activation and lipid binding (*12*−*14*). The C-terminal domain (residues 187−243) is highly hydrophobic and is proposed to contain the primary lipid binding site in apoA-I (*15*, *16*). Several models of the secondary structure of lipid-free apoA-I have been built on the basis of these findings (*10*, *17*, *18*).

The crystal structure of apoA-I Δ(1−43) at 4 Å resolution (*19*) that is proposed to mimic the lipid-bound protein conformation shows 10 amphipathic α-helical repeats forming a sharply curved "horseshoe" shape that places the N- and C-termini only 23 Å apart. The proximity of N- and C-termini has also been suggested in other studies of lipid-free apoA-I (*11*, *20*, *21*).

The focus of this work is on the central region of apoA-I. A series of terminal deletion mutants were expressed by mutagenesis: Δ(1−41), truncation near the start position of exon 4; Δ(1−59), truncation to the first predicted amphipathic α-helix in the model of Nolte and Atkinson (*10*);

† This work was supported by Grants POHL26335 and HL48739 from the National Institutes of Health.

* To whom correspondence should be addressed. Phone: (617) 638-4015. Fax: (617) 638-4041. E-mail: atkinson@bu.edu.

[1] Abbreviations: apo, apolipoprotein; CD, circular dichroism; HDL, high-density lipoprotein(s); LCAT, lecithin:cholesterol acyltransferase; SR-BI, scavenger receptor class B type I; rTEV protease, recombinant tobacco-etched viral protease; MWCO, molecular weight cutoff; Ni-NTA, nickel nitrilotriacetic acid; SDS−PAGE, sodium dodecyl sulfate−polyacrylamide gel electrophoresis; IEF, isoelectric focusing.

10.1021/bi034152t CCC: $25.00
Published on Web 05/13/2003

Δ(1−41, 185−243) and Δ(1−59, 185−243), deletions of both N- and C-terminal parts. We carried out structural and thermal unfolding studies of these mutants and analyzed the effects of pH on the protein conformation.

MATERIALS AND METHODS

Protein Expression and Purification. The C-terminal deletion mutants Δ(198−243) and Δ(209−243) were expressed in mouse mammary tumor cell line C127 as described before (*22*). The proteins were secreted to the cell culture media and purified by FPLC using ion-exchange column (HiTrapQ, Pharmacia) and gel-filtration column chromatography. After several harvests, the collected media were concentrated to 50 mL using an Amicon ultrafiltration cell with YM10 membrane [molecular weight cutoff (MWCO) = 10 K]. The concentrated media were dialyzed against 0.01 M Tris buffer at pH 8, filtered, and passed through an ion-exchange column (HiTrapQ, 5 mL, Pharmacia). The protein was eluted with a step gradient (0% → 5% → 60% → 100%) of 1 M NaCl in 0.01 M Tris, pH 8. The elution fractions were checked for apoA-I by sodium dodecyl sulfate−polyacrylamide gel electrophoresis (SDS−PAGE). The fractions containing apoA-I were pooled and concentrated to <2 mL using a Centricon 10 (or Centriprep, Amicon) with a membrane of MWCO = 10 K. The sample was then applied to a gel-filtration column (HiPrep 26/60, Sephacryl S-100). The elution buffer was 0.15 M NaCl, 0.01 M Tris, and 0.02% NaN_3, pH 8; the elution rate was 0.1 mL/min. The eluted fractions and the purity were assessed by 12.5% SDS−PAGE. Fractions with pure apoA-I were collected for further studies. Proteins obtained from the C127 cell line contain the additional Arg-His-Phe-Trp-Gln-Gln- propeptide at the N-terminus.

The N-terminal deletion mutants, Δ(1−41) and Δ(1−59), and the double N- and C-terminal deletion mutants, Δ(1−41, 185−243) and Δ(1−59, 185−243), were expressed as His-tagged proteins in the insect cell line Sf-9 as described before (*18*). The cells were sonicated, and the proteins in the supernatant were purified by using nickel nitrilotriacetic acid (Ni-NTA) resin from Qiagen Inc. The 6 × His tag that was attached to the amino terminus allowed the immobilization of the protein on metal-chelating surfaces such as Ni-NTA. The NTA ligand is sufficient for the binding of 5−10 mg of 6 × His-tagged protein/mL of Ni-NTA resin. To cleave off the His tag, the construct also included an additional 24-residue recombinant tobacco-etched viral (rTEV) protease recognition site. The His tag was enzymatically removed after purification, and the separation of the non-His-tagged apoA-I from the His-tagged rTEV enzyme was achieved by using Ni-NTA resin. The purified apoA-I was analyzed by 12.5% SDS−PAGE (Figure 1), and the concentration was determined by Lowry assay. The proteins obtained from Sf-9 cells have an additional Gly-Ala-Met-Gly-Ser- at the N-terminus that results from the residual rTEV protease cleavage site.

Circular Dichroism (CD) Spectroscopy. The CD spectra were measured with an upgraded Aviv 62DS spectropolarimeter equipped with thermoelectric temperature control (Aviv Associates, Lakewood, NJ). Solutions of ∼0.06−0.10 mg/mL protein concentrations in 10 mM PBS (pH 4.7−7.8) were placed in 1−2 mm quartz cuvettes for far-UV experiments (wavelengths 185−250 nm), and solutions of 0.1−0.4 mg/mL protein concentrations were used in 5−10 mm cuvettes for near-UV experiments (250−320 nm). The spectra were recorded every 1 nm, with 15−30 s accumulation time per data point, and averaged over three to five runs. After buffer baseline subtraction, the CD data were normalized to protein concentration and are expressed as molar residue ellipticity in far-UV CD and as molar ellipticity in near-UV CD. ORIGIN software (Microcal, Amherst, MA) was used for the CD data display and analysis.

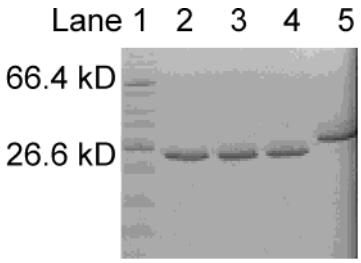

FIGURE 1: SDS−PAGE showing the purified wild-type apoA-I after rTEV cleavage: lane 1, molecular mass markers; lanes 2−4, pure non-His-tagged apoA-I after rTEV reaction; lane 5, His-tagged apoA-I before rTEV reaction.

Protein α-helical content was determined with 5% accuracy from the measured molar residue ellipticity at 222 nm, $[\Theta_{222}]$, according to (*23*)

$$\% \ \alpha\text{-helix} = (-[\Theta_{222}] + 3000)/39000$$

CD Analysis of Thermal Unfolding. Protein unfolding was monitored by the CD signal $\Theta_{222}(T)$ at 222 nm upon sample heating from 5 to 95 °C at a rate of 0.6−1.0 K/min, with 0.5−1 °C increment and 60−90 s accumulation time per data point. CD melting data indicative of a cooperative thermal unfolding were used to determine the melting temperature T_m and van't Hoff enthalpy $\Delta H_v(T_m)$ by a conventional van't Hoff analysis (*24*). In such an analysis, the baselines for the folded and unfolded states, $[\Theta_F]$ and $[\Theta_U]$, were determined by linear extrapolation from the pre- and posttransitional regions of the thermal unfolding curve. The equilibrium constant K_{eq} in the transitional region was determined from the experimentally measured ellipticity $[\Theta_{222}]$ as

$$K_{eq} = [U]/[F] = ([\Theta_{222}] - [\Theta_F])/([\Theta_U] - [\Theta_{222}])$$

Van't Hoff plots, ln K_{eq} versus $1/T$, were nearly linear, indicating a small heat capacity increment associated with the apoA-I unfolding, which is consistent with our calorimetric data (*25*). Linear fitting of the van't Hoff plots was used to determine the values of T_m and ΔH_v according to the van't Hoff equation:

$$\ln K_{eq} = -(\Delta H/R)(1/T) + (\Delta S/R)$$

Here $R = 1.987$ cal/mol is the universal gas constant, and T is temperature in Kelvin. The slope of the linear function provides the value of ΔH, and the X-axis intercept corresponds to $1/T_m$, where T_m is the melting temperature. The value of T_m was also determined from the peak position in the first derivative function $d[\Theta_{222}(T)]/dT$ (*26*).

Isoelectric Focusing Gel Electrophoresis. Isoelectric focusing (IEF) was used to separate the proteins according to their isoelectric points, p*I*. The IEF gels were premade ready-

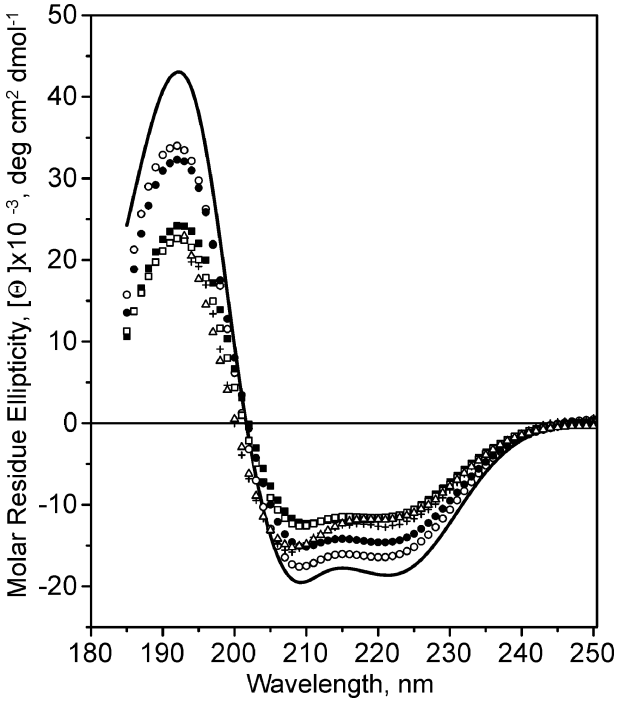

FIGURE 2: Far-UV CD spectra of variant apoA-I forms at pH 7.8 and 25 °C: (—) wild type, (■) Δ(1−41), (●) Δ(1−59), (□) Δ(1−41, 185−243), (○) Δ(1−59, 185−243), (Δ) Δ(198−243), and (+) Δ(209−243). The samples contained 0.1 mg/mL protein in 0.01 M PBS.

to-use phast gels purchased from Pharmacia (Amersham Pharmacia Biotech, Piscataway, NJ) with a p*I* gradient of 3−9 (wide range) or 4.5−6 (narrow range). Markers used were broad p*I* 3.5−9.3 (for wide-range gel) and low p*I* 2.8−6.5 (for narrow-range gel). Coomassie blue (0.1%) was used for staining. The destain solution was 30% methanol and 10% acetic acid, and the preserving solution was 5% glycerol in 10% acetic acid.

RESULTS

Secondary Structure and Thermal Unfolding of Variant ApoA-I Forms at pH 7.8. The lipid-free wild-type apoA-I and terminally truncated apoA-I mutants Δ(1−41), Δ(1−59), Δ(1−41, 185−243), and Δ(1−59, 185−243) obtained from Sf-9 cells, as well as the Δ(198−243) and Δ(209−243) mutants obtained from C127 cells, were analyzed by CD spectroscopy at near-physiological solvent conditions (10 mM PBS, pH 7.8). Figure 2 shows the far-UV CD spectra recorded from these proteins at 25 °C. The spectra exhibit negative peaks at 222 and 208 nm and a positive peak at 193 nm, which are characteristic of an α-helix. Thus, the dominant secondary structure in the wild-type and the mutant proteins is α-helix, regardless of the deleted portion of the protein.

The protein α-helical content, which was estimated on the basis of the CD intensity at 222 nm, is listed in Table 1. The data in Figure 2 and Table 1 show that the α-helical content of the mutant proteins is 37−52%, lower than the 55% α-helical content in the wild type and 60% in plasma apoA-I (*27*, *28*). The N-terminal deletion mutants Δ(1−41) and Δ(1−59) have a similar number of residues in the α-helical conformation (83 and 85 ± 8, respectively), suggesting that the α-helical structure in these two mutants is similar. Therefore, in the Δ(1−41) mutant, residues 42−59 are probably unfolded, and the slightly higher percent α-helical content in Δ(1−59) compared to Δ(1−41) may result simply from the deletion of the segment 42−59 that is nonhelical in the Δ(1−41) mutant.

Table 1: α-Helical Composition of Variant ApoA-I Forms

	α (%)[a]	total no. of protein residues/ residues in α-helices[b]	residues deleted/ residues lost from α-helices[b,c]
plasma	60[d]	243/146	0
WT^{Sf9} [e]	55	248/136	0
Δ(1−41)^{Sf9}	40	207/83	41/63[g]
Δ(1−59)^{Sf9}	45	189/85	59/61
Δ(1−41, 185−243)^{Sf9}	37	148/55	100/91
Δ(1−59, 185−243)^{Sf9}	52	130/67	118/79
Δ(198−243)^{C127} [f]	40	203/81	46/65[g]
Δ(209−243)^{C127}	40	214/86	35/61[g]

[a] The α-helical content is the mean value derived from three to five independent measurements of three to five different samples. The error in this estimate is ∼5%. [b] ±8 residues. [c] Compared to plasma apoA-I. [d] From refe *25*. [e] Proteins obtained from the Sf-9 cell line. [f] Proteins obtained from the C127 cell line. [g] ApoA-I mutants in which the deletions lead to α-helical unfolding in other parts of the molecule.

In the N-terminal single deletion mutant Δ(1−41) and in the single C-terminal deletion mutants Δ(198−243) and Δ(209−243), the reduction in the number of residues in the α-helical structure resulting from the mutations is significantly greater than the number of deleted residues (footnote *g* in Table 1). This indicates that the deletion of a single N- or C-terminal segment leads to major α-helical unfolding (∼60 residues) elsewhere in the molecule. Interestingly, the number of residues in helical conformation in each of the mutants is similar (81−86 residues). This perhaps indicates a core helical domain of ∼85 residues in the protein.

In contrast, in double deletion mutants Δ(1−41, 185−243) and Δ(1−59, 185−243), the reduction in the number of helical residues resulting from mutation is much smaller than the total number of deleted residues. Therefore, the reduction in the α-helical content in these mutants may be accounted for, at least in part, by deletion of helical segments. However, the resulting helical content is less than that expected if all remaining 11/22 tandem repeat units were in helical conformation, indicating that additional regions of these mutants are unfolded. Interestingly, the Δ(1−59, 185−243) mutant appears to have ∼12 residues greater helical content than Δ(1−41, 185−243), suggesting that some part (possibly one 11-mer) in the central core domain of residues 60−185 refolds to helix in the absence of segment 42−59. A similar observation was made in previous studies of the C-terminal deletion mutant Δ(185−243) (*22*).

The thermal unfolding data of apoA-I variants at pH 7.8 recorded by CD at 222 nm are shown in Figure 3. The melting curves $[\Theta_{222}](T)$ show that the protein secondary structure is nearly invariant from 0 °C to near-physiological temperatures. The unfolding of the α-helical structure is observed from about 40 to 80 °C, with midpoint T_m between 50 and 60 °C, close to T_m ∼57 °C of plasma apoA-I (*25*). At 70 °C, most of the α-helical protein structure is unfolded. The unfolding transition is reversible, as indicated by a complete superimposition of the melting curves recorded at various scan rates from 0.6 to 1 K/min.

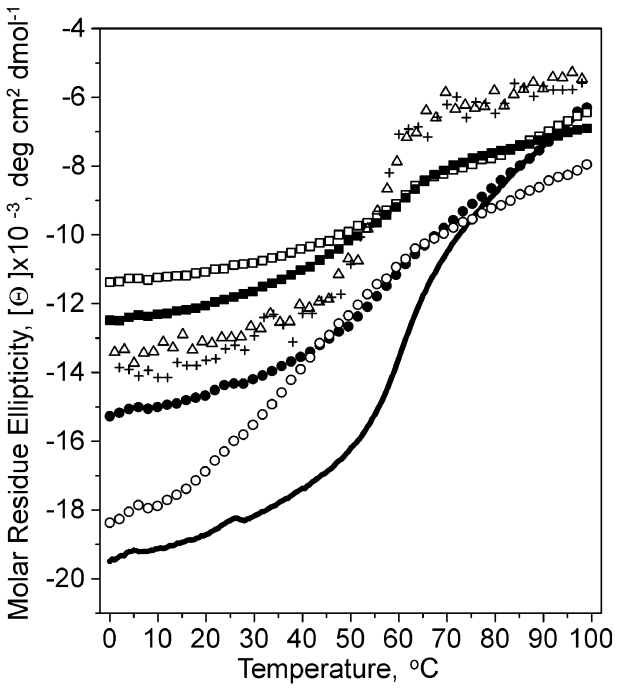

FIGURE 3: Heat unfolding of variant apoA-I forms at pH 7.8 monitored by CD at 222 nm: (—) wild type, (■) Δ(1−41), (●) Δ(1−59), (□) Δ(1−41, 185−243), (○) Δ(1−59, 185−243), (Δ) Δ(198−243), and (+) Δ(209−243). The samples contained 0.1 mg/mL protein in 0.01 M PBS.

The heat unfolding curves in Figure 3 show that the C-terminal deletion mutants Δ(198−243) and Δ(209−243) still form reasonably cooperative structures, as also shown previously (*22*). However, N-terminal truncations [including Δ(1−41), Δ(1−59), Δ(1−41, 185−243), and Δ(1−59, 185−243)] lead to a large reduction in the unfolding cooperativity that precludes van't Hoff analysis. This suggests that the deletion of the first 41 residues in apoA-I, which is common to all of these mutants, leads to changes in the overall molecular structure, resulting in a less cooperative unfolding.

pH Effects on the Secondary Structure and Thermal Unfolding of Variant ApoA-I Forms. Figure 4 shows the far-UV CD spectra and the melting curves of variant apoA-I forms at pH 4.7 and 7.8, 25 °C. The shapes of the far-UV CD spectra at pH 4.7 and 7.8 are similar, indicating that the dominant secondary structure is α-helical over this pH range. In contrast to the wild-type apoA-I whose helical content remains invariant in the pH range analyzed (Figure 4A), all mutant proteins show a marked increase in the α-helical content upon reduction in pH from 7.8 to 4.7 (Figure 4B−E). For example, mutant Δ(1−59, 185−243) contains 52% α-helix at pH 7.8, 60% α-helix at pH 6.5, and 70% α-helix at pH 4.7 (Figure 4E). Other apoA-I mutants show smaller but significant increases in their α-helical content upon reduction in pH from 7.8 to 4.7.

The insets in Figure 4 show thermal unfolding data recorded from apoA-I variants at pH 7.8 and 4.7. These data clearly show that the reduction in pH from 7.8 to 4.7 leads to a significant increase in the thermal unfolding cooperativity, thereby facilitating van't Hoff analysis. Figure 5 shows the van't Hoff plots for the heat unfolding of apoA-I variants at pH 4.7 that are based on the thermal unfolding data in Figure 4. The melting temperatures T_m determined from the van't Hoff plots are in good agreement with the values determined from the peak positions in the first derivative functions, $d[\Theta_{222}(T)]/dT$, of the thermal unfolding data (insets in Figure 5). The values of T_m and the van't Hoff enthalpies ΔH_v are summarized in Table 2. These values show that Δ(1−59, 185−243) has a significantly higher T_m at pH 4.7 compared to other mutants.

In summary, the results in Figures 4 and 5 and Table 2 indicate that a reduction in pH from 7.8 to 4.7 leads to a significant increase in the α-helix content of the apoA-I mutants by 7−20% and to a large increase in their thermal unfolding cooperativity.

Near-UV CD Spectra of ApoA-I: Effects of Mutations, Protein Concentrations, and pH. Near-UV CD spectra of the variant forms of apoA-I are shown in Figure 6. As apoA-I lacks Cys residues, the major contribution to its near-UV CD comes from the aromatic side chains. Wild-type apoA-I contains four Trp (W8, 50, 72, 108), seven Tyr (Y18, 29, 100, 115, 166, 192, 236), and six Phe (F33, 57, 71, 104, 225, 229). Its near-UV CD spectrum at pH 7.8 (Figure 6A) shows a large negative peak at 295 nm that corresponds to the L_β transition of Trp and a smaller peak at 285 nm that may have contributions from the L_β transitions of Tyr and of Trp. The spectrum of the wild type is similar to that of plasma apoA-I in solution (*25*, *29*), suggesting similar Trp and Tyr packing in these proteins. The spectra recorded from wild-type apoA-I at 0.1 mg/mL (where the protein is predominantly monomeric) and at 0.2−0.3 mg/mL [where apoA-I is partially self-associated (*30*, *31*)] closely overlap (Figure 6A), indicating that the near-UV CD spectrum of wild-type apoA-I does not result from the protein quaternary interactions and thus arises from its tertiary packing.

The terminal deletions of apoA-I lead to significant changes in the near-UV CD (Figure 6). In contrast to the near-UV CD of wild-type apoA-I, the spectra of all mutants show a large broad positive peak extending from 260 to 280 nm (Figure 6B−E). This peak may correspond to the L_α transition of Trp that is particularly sensitive to the environmental conditions (*32*, *33*). Since all apoA-I mutants that show this large near-UV CD peak have the first 41 residues deleted, this deletion may provide the common origin of the observed spectral changes. The removal of one Trp, two Tyr, and one Phe that are located in the deleted 1−41 segment is unlikely to lead to the observed increase in the spectral intensity of the mutant proteins. Therefore, the changes in the near-UV CD of the apoA-I mutants probably result from tertiary and/or quaternary structural changes induced by the N-terminal deletion.

The protein concentration has little effect on the near-UV CD of the wild-type apoA-I (Figure 6A) but has a significant effect on the spectra of the mutant proteins (Figure 6B−E). For the N-terminal or double N- and C-terminal deletion mutants, the near-UV CD spectra at different protein concentrations largely overlap at $\lambda > 280$ nm. However, at shorter wavelengths, the amplitude of the large peak between 260 and 280 nm decreases as the protein concentration decreases, and the peak position shows a red shift, from 265 nm at 0.3 mg/mL to 270 nm at 0.1 mg/mL (Figure 6B−E). Therefore, this peak may have a significant contribution from the protein self-association. Such a concentration dependence suggests that the deletion of the 41 N-terminal residues induces large changes in the self-association properties of apoA-I.

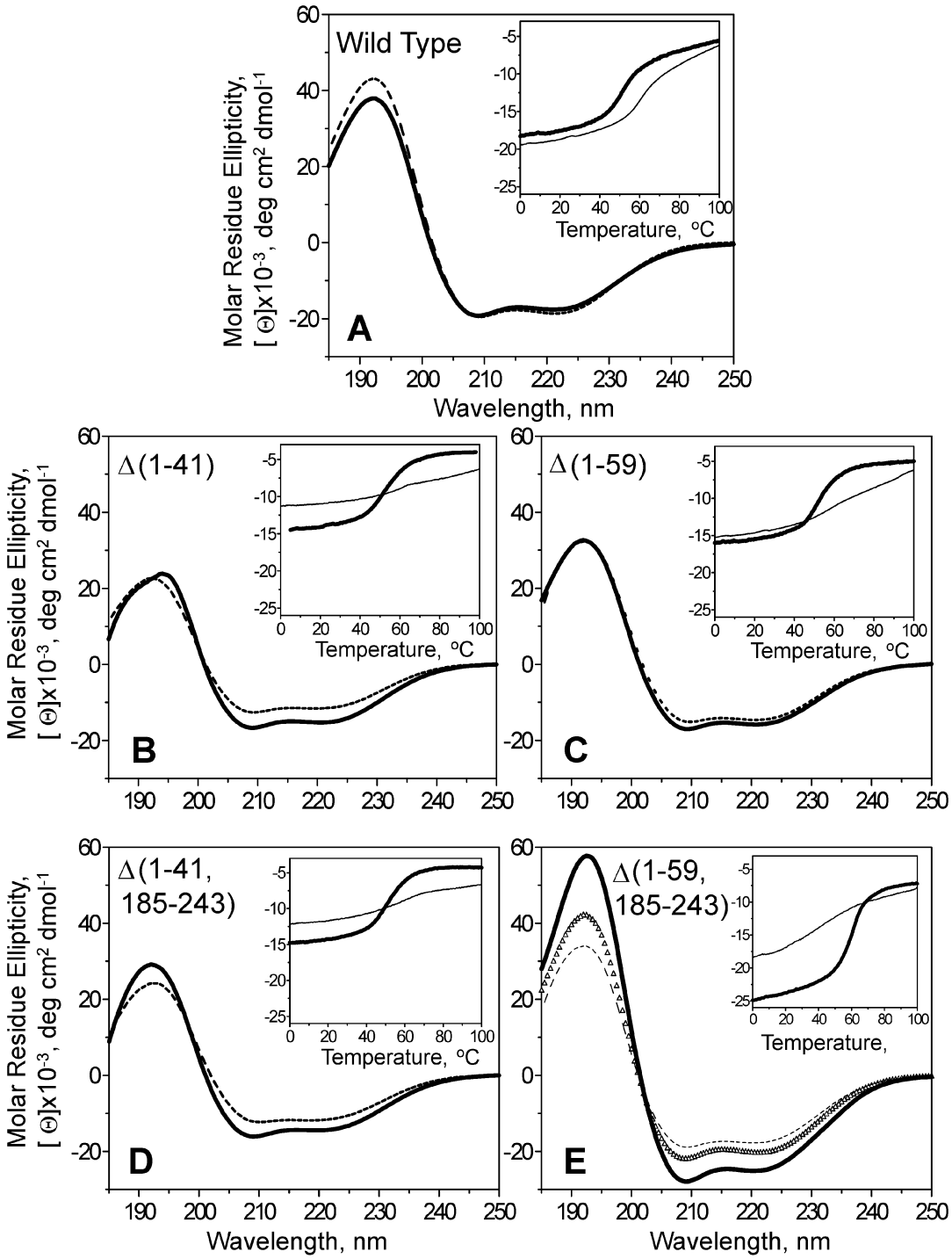

FIGURE 4: pH effects on far-UV CD spectra of variant apoA-I forms: (---) pH 7.8, (Δ) pH 6.5, and (—) pH 4.7. Insets: Heat unfolding curves of apoA-I variants at (—) pH 7.8 and (**—**) pH 4.7.

The near-UV CD spectra of apoA-I variants are significantly affected by pH. The spectra of the wild-type apoA-I show a reduction in the CD intensity at wavelengths below 280 nm upon reduction in pH from 7.8 to 4.7 (Figure 6A). Such spectral changes in the L_α region of Trp suggest tertiary/quaternary structural changes and/or changes in the electrostatic environment of Trp residues that may occur in this pH range. For the mutant proteins with the exception of Δ(1−59, 185−243), the pH-induced changes in the near-UV CD are even more pronounced, and the large positive peak at 260−280 nm observed at pH 7.8 is not exhibited at pH 4.7 (Figure 6B−D). The overall shape of the mutant spectra at pH 4.7 becomes similar to that of the wild type at the same pH. This suggests that, in contrast to pH 7.8, at pH 4.7, wild-type and these mutant apoA-I have similar tertiary and quaternary structures. Mutant Δ(1−59, 185−243) shows a different near-UV CD spectrum at pH 4.7 compared to the other mutants (Figure 6E). In addition, far-UV CD data indicate that at pH 4.7 this mutant has significantly higher α-helical content (70%), melting temperature (T_m = 59 °C), and thermal unfolding cooperativity (Figure 4, Table 2) than the other mutants. The values are similar to those of wild-type apoA-I at pH 7.8. Taken together, our far- and near-UV CD data at pH 4.7 suggest a

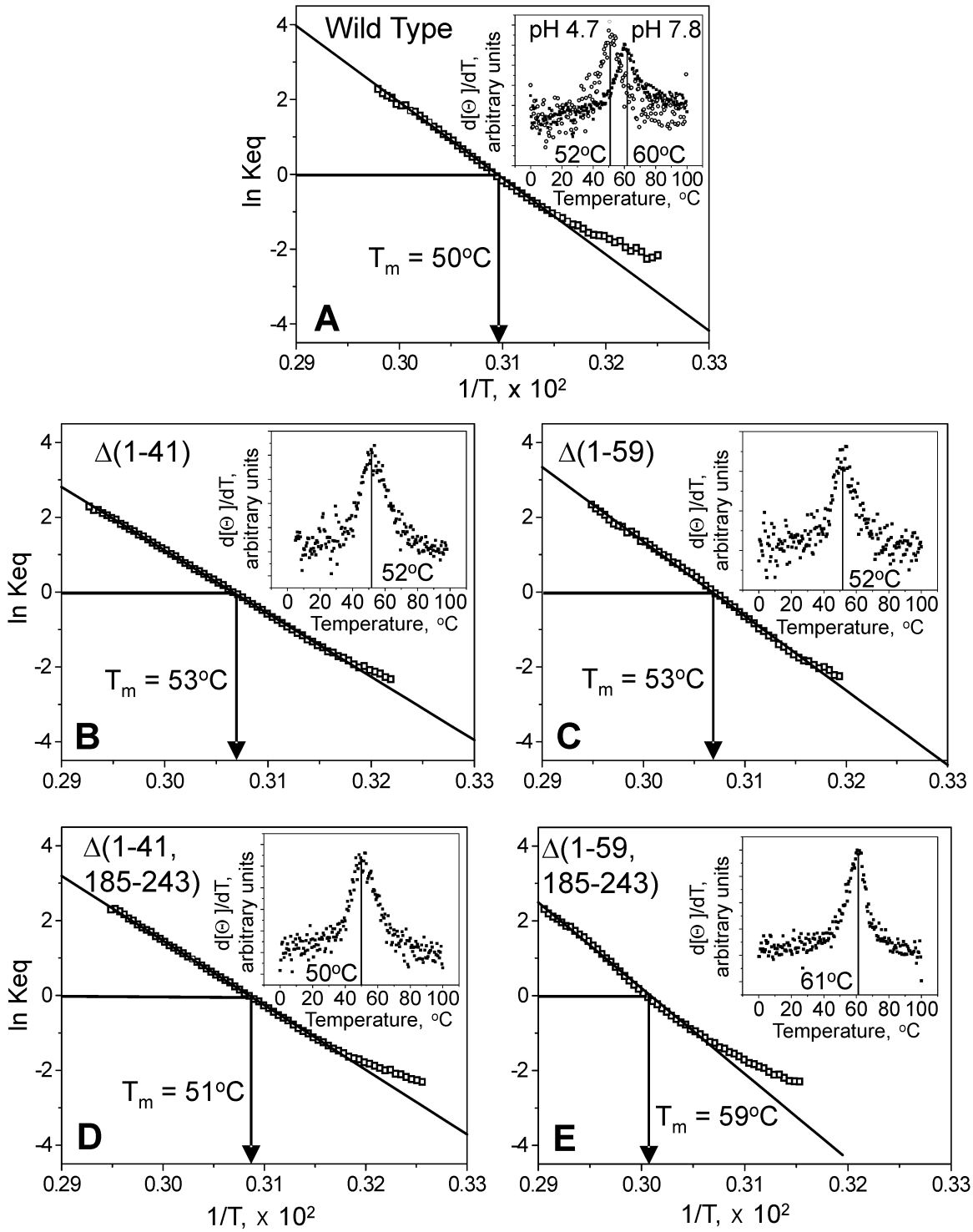

FIGURE 5: Van't Hoff plots ln K_{eq} versus 1/T for the apoA-I variants at pH 4.7. The plots are based on the thermal unfolding data $[\Theta_{222}](T)$ shown in Figures 3 and 4. Arrows indicate the melting temperatures. Insets: First derivative functions $d[\Theta_{222}]/dT$ of the thermal unfolding data.

substantially different conformation for Δ(1−59, 185−243) compared to other mutants.

DISCUSSION

Roles of the N- and C-Termini in the Overall Conformation of Lipid-Free ApoA-I. The results of our CD studies show that in all of the single N- or C-terminal deletion mutants analyzed, including Δ(1−41), Δ(1−59), Δ(198−243), and Δ(209−243), the reduction in the number of residues in the α-helical conformation resulting from mutations exceeds the number of deleted residues (footnote *g* in Table 1). This implies that the deletion of a single N- or C-terminal segment leads to α-helical unfolding elsewhere in the molecule. We hypothesize that the N- and C-terminal regions interact with each other in intact apoA-I; thus the deletion of either of the terminal regions leads to the helical unfolding in the remaining terminus. This is consistent with the observation that in double deletion mutants, Δ(1−41, 185−243) and Δ(1−59, 185−243), the reduction in the number of residues in the helical conformation resulting from

Table 2: Structural and Thermodynamic Properties of ApoA-I[a]

	α-helical content (%)[b]		no. of residues in α-helices at pH 4.7/ no. increased at pH 4.7 compared to pH 7.8[c]	T_m (°C)[d]		ΔH_v (kcal/mol)[e]
	pH 7.8	pH 4.7		pH 7.8	pH 4.7	pH 4.7
wild type	55	55	136/0	60	50	39
Δ(1−41)	40	47	97/14		53	32
Δ(1−59)	45	48	91/6		53	36
Δ(1−41, 185−243)	37	44	65/10		51	36
Δ(1−59, 185−243)	52	70	91/24		59	40

[a] The melting temperature T_m and van't Hoff enthalpy ΔH_v were determined from van't Hoff analyses of the heat unfolding at pH 4.7 in Figures 3 and 4. [b] ∼5% error. [c] ±8 residues. [d] ∼2 °C error for wild-type apoA-I at pH 7.8 and 4.7 and apoA-I variants at pH 4.7; for apoA-I variants T_m at pH 7.8 could not be determined because of the low cooperativity of the thermal unfolding. [e] ∼4−5 kcal/mol error.

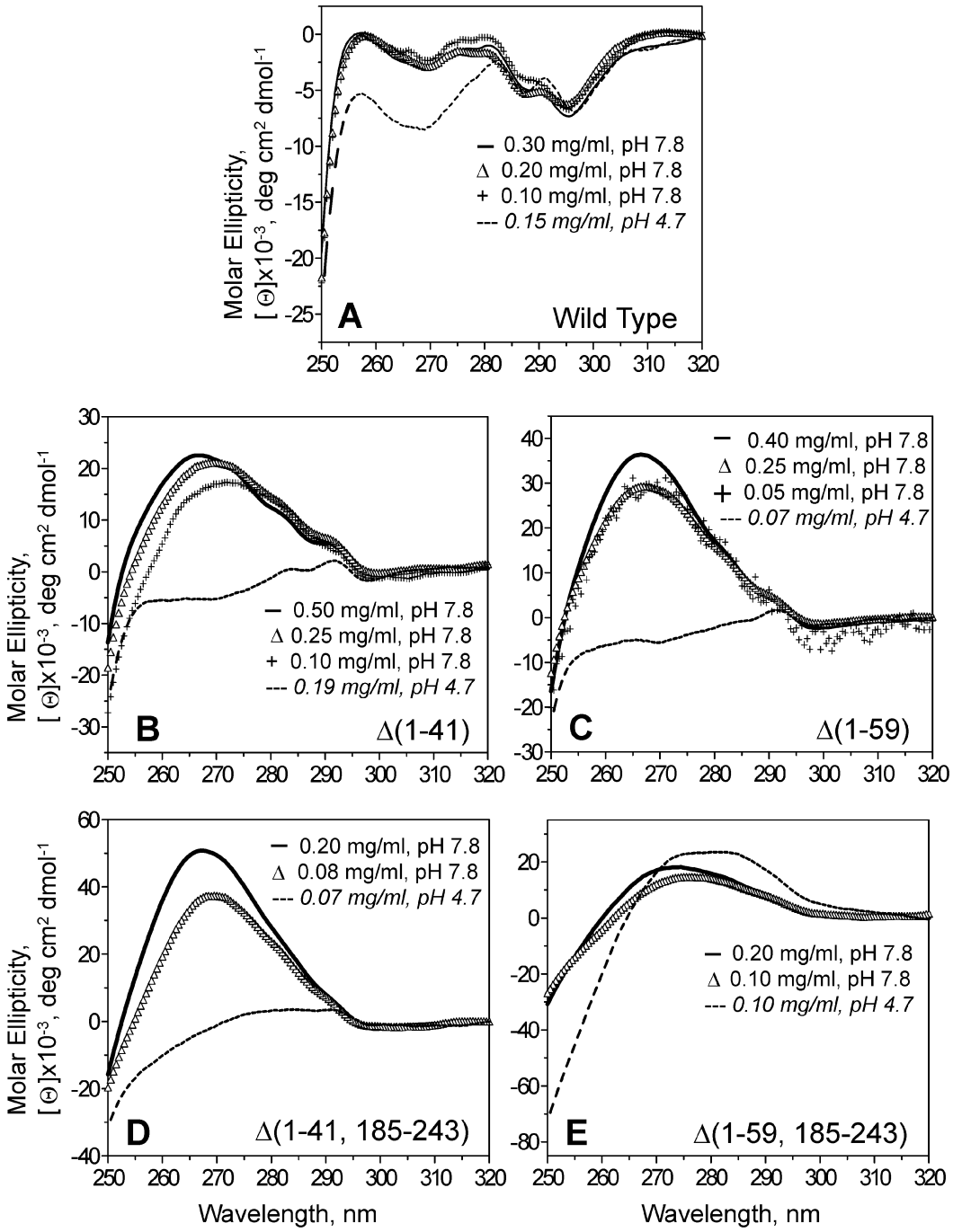

FIGURE 6: Effects of protein concentration and pH on near-UV CD spectra of apoA-I. Protein concentrations and pH are indicated.

mutation is much smaller than the total number of the deleted residues (Table 1). Therefore, the reduction in the α-helical content in these mutants can be accounted for by deletion of the helical segments from the N- and C-terminal parts

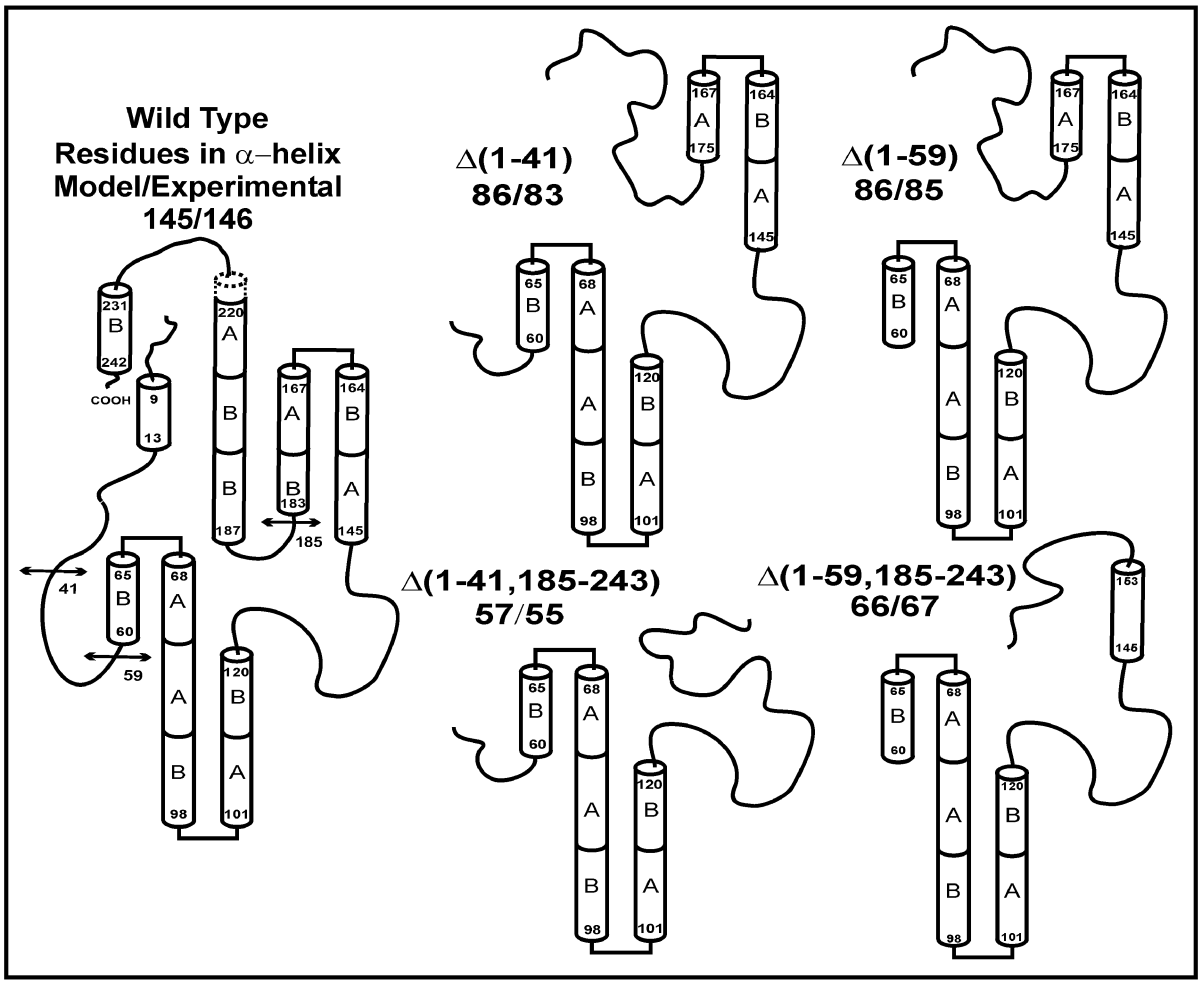

FIGURE 7: Secondary structure models for wild-type and N- and C-terminally truncated apoA-I. The model for wild type (left) incorporates secondary structure elements that were predicted on the basis of amino acid sequence analysis (*10*), as well as the results of mutational studies suggesting the helical structure in the C-terminal region (*22*) and the unfolded conformation for the 122−144 segment in solution (*18*). The model incorporates the juxtaposition of the N- and C-termini as suggested in this study. Sites of the mutations studied in the current work are indicated (↔). For the wild type and each mutant, the number of amino acids in α-helical conformation in the model and that derived from CD spectroscopy (Table 1) are indicated. The helical regions are shown as cylinders with the N- and C-terminal residues indicated. A and B in the models indicate type A and B 11-mer amino acid repeats.

and must also involve the helical unfolding in other parts of the molecule. In summary, our results indicate that, in intact apoA-I in solution, the N- and C-terminal segments are involved in the intramolecular stabilizing interactions and may possibly interact with each other to maintain the overall structure of the apoA-I protein.

Since the central part of apoA-I has been consistently predicted to comprise a well-defined α-helical region, while the termini have less well-defined structure, the deletion of the terminal portions might be expected to result in a better ordered more cooperative structure. Contrary to this expectation, our CD results show that the deletion mutants have lower helical content and lower thermal unfolding cooperativity (Figures 2 and 3, Table 1). Consequently, the intramolecular interactions involving the N- and C-terminal parts of the molecule are essential for maintaining the integrity and the cooperativity of the solution structure of apoA-I.

On the basis of the CD spectroscopic analysis of the N- and C-terminal deletion mutants of apoA-I reported in this work, we propose putative secondary structural models of these mutants as shown in Figure 7. The model for wild-type apoA-I incorporates secondary structure elements (such as α-helices or turns) that were predicted on the basis of the amino acid sequence analysis (*10*), as well as the results of our recent mutational studies suggesting the helical structure in the C-terminal region (*22*) and the unfolded conformation for the 122−144 segment in solution (*18*). We have modified this model to incorporate the juxtaposition of the N- and C-termini that is suggested by the results of this and other studies (*11*, *20*, *21*). The α-helical structure in each of the models in Figure 7 corresponds to the numbers of amino acids in α-helical conformation determined by CD spectroscopy (Table 1). These models are also consistent with results of the deletion studies from other groups (*34*), suggesting that a substantial fraction of the helical structure in lipid-free apoA-I resides in its N-terminal part (residues 44−126).

Comparison of the model structures of the N-terminal deletion mutants Δ(1−41) and Δ(1−59) in Figure 7 shows that the deletion of the 42−59 segment that is unfolded in Δ(1−41) does not alter the secondary structure in other parts of the molecule, which is consistent with the results of our CD analysis. Similarly, the deletion of the 42−59 segment in the context of the double deletion mutants Δ(1−41, 185−243) and Δ(1−59, 185−243) may lead to secondary structural changes in the remaining 145−184 region, perhaps in

the short 145−153 segment, but not in other parts of the molecule (Figure 7). Furthermore, comparison of the model structures of the corresponding single and double deletion mutants, such as Δ(1−41) and Δ(1−41, 185−243), shows that the deletion of the C-terminal segment (185−243) leads to helical unfolding in the adjacent 145−175 segment. The unfolding in this segment is also evident from the comparison of the model structures of Δ(1−59) and Δ(1−59, 185−243) mutants. In summary, the model structures of apoA-I deletion mutants illustrated in Figure 7 are consistent with the results of our CD analysis of these mutants, as well as the earlier structural studies of apoA-I from our laboratory and from other groups.

Interestingly, our results are different from some other earlier studies of similar terminal deletion mutants of apoA-I. These studies showed no significant structural changes induced by the C-terminal deletion Δ(187−243) (*11*, *22*) but revealed large secondary and tertiary structural changes resulting from the N-terminal deletion Δ(1−43) (*11*, *35*). The Δ(1−43) apoA-I mutant had an increased α-helical content (∼82%) and other structural characteristics that were suggested to indicate that the solution conformation of this mutant mimics the lipid-bound protein conformation. The difference between these earlier studies and our data on Δ(1−41) and Δ(1−59) may result from the difference in the exact size of the deleted fragment, and/or from the difference in the protein source, or the presence of extra five residues at the N-terminus of the proteins analyzed in our work.

Effects of pH on the Structure of ApoA-I. The most significant and novel result of this study is the large changes in the solution structure of the apoA-I variants induced by changes in pH from 7.8 to 4.7 (Figures 4 and 6). To understand the origin of these pH-induced structural changes, we used isoelectric focusing (IEF) gels to determine the p*I* values of the proteins under study. The IEF gels indicate p*I* = 5.2 for the wild-type apoA-I (compared to p*I* ∼ 5.2 of plasma apoA-I,), p*I* = 5.6 for the N-terminal deletion mutants, and p*I* = 4.7 for the double N- and C-terminal deletion mutants (data not shown).

The effects of pH on the protein secondary structure and unfolding cooperativity observed in our work may result from the reduction in the net negative charge on the protein at pH 4.7 compared to pH 7.8. Such a charge reduction may reduce the electrostatic repulsion between individual helical segments, leading to the observed increase in the α-helical content and thermal unfolding cooperativity.

The p*I* values of individual amphipathic α-helices, which are calculated on the basis of the amino acid composition and assuming normal p*K* for the ionizable groups, show that despite the general similarity in the amino acid composition of individual α-helices in apoA-I, these helices have very different calculated p*I* ranging from 4.14 to 8.49. Therefore, in the pH range under study, the net charge on different helices may have different sign. For example, at pH 7.8, helices 66−87 (p*I* 4.14), 88−98 (p*I* 6.18), and 99−120 (p*I* 4.80) all have negative net charge, yet the net charge on helices 121−142 (p*I* 7.19) and 143−164 (p*I* 7.34) is close to zero. Upon the reduction in pH to 4.7, the net charge on helix 88−98 changes sign to positive, helices 66−87 and 99−120 become near neutral, and helices 121−142 and 143−164 become positively charged. This change in the net charge of individual α-helices may lead to changes in the interhelical interactions, resulting in the observed pH-induced conformational changes in apoA-I. Some earlier studies have also shown that the mutation of charged residues E → K induces helix formation in apoA-I (*18*).

In addition to the observed secondary structure changes, the near-UV CD studies of the apoA-I variants show that the tertiary and/or quaternary protein structures are also significantly affected by the mutations, protein concentration, and pH (Figure 6). This further supports our conclusion that the terminal regions of apoA-I play an important role in stabilizing the overall protein conformation.

The pH-induced structural changes revealed in this work may be relevant to the conformational changes in apoA-I that occur upon lipid binding. Indeed, the local pH near the phospholipid membrane may be significantly lower than the neutral pH in plasma (*36*); similarly, a local reduction in pH may occur at the lipoprotein surface that is comprised of neutral and anionic phospholipid headgroups. Thus, the increase in the α-helical content accompanied by the tertiary and/or quaternary structural changes at pH 4.7 in lipid-free apoA-I and its terminal deletion mutants revealed in our work may resemble aspects of the protein conformational adaptability that are key to its association with lipoproteins.

Unfolding Cooperativity and Helix Pairing in ApoA-I. The van't Hoff enthalpies ΔH_v determined in our thermal unfolding studies of lipid-free wild-type apoA-I at pH 4.7−7.8 and of the deletion mutants at pH 4.7 range from 32 to 40 kcal/mol. This range encompasses the values determined for plasma apoA-I by CD (32 kcal/mol) and by differential scanning calorimetry (∼40 kcal/mol) (*25*), as well as the values of ΔH_v determined by CD for other point and deletion mutants of apoA-I (*22*). As the value of ΔH_v corresponds to the heat of unfolding of an average cooperative unit, this similarity in ΔH_v indicates similar average size of the cooperatively unfolding unit in these apoA-I variants.

Earlier, we suggested that the cooperative unit in apoA-I is comprised of an amphipathic α-helix formed from one 22-mer repeat (*25*). We now reevaluate this assessment and propose that the cooperative unit in apoA-I and its variants contains a pair of such helices connected by a linker. Indeed, a characteristic 22-mer repeat from the central part of apoA-I is predicted to form an α-helix of ≤8 amino acids that is connected via a ≥4-residue linker to the adjacent helical segments. In solution, a pair of such helices may form a helix hairpin, with ≤36 residues in an α-helical conformation. The enthalpy of unfolding of such a helical structure is expected to be ∼40 kcal/mol, assuming the enthalpy of 1−1.3 kcal/mol residue measured for the helix-to-coil transition in solution (*37*). The good agreement between this value and the van't Hoff enthalpies determined for apoA-I variants in this and in the earlier studies (*22*, *25*) suggests that the cooperative unit in these proteins consists of one helix pair comprised of two 22-mer sequence repeats.

Helix pairing has been proposed to play an important structural and functional role in other apolipoproteins, such as apoE (*38*), apoC-I (*39*), and apolipophorin III (*40*). Our results corroborate these earlier data and suggest that a helix pair may represent a cooperatively folded structural unit in apoA-I and in other exchangeable apolipoproteins.

ACKNOWLEDGMENT

We are grateful to Dr. Vassilis I. Zannis and Dr. Tong Liu for the collaboration in the apoA-I mutant expression systems. We thank Cheryl England for help in the biochemical experiments and Dr. Elena Klimtchuk for very useful discussions of the near-UV CD spectra.

REFERENCES

1. Castelli, W. P., Doyle, J. T., Hames, C. G., Hjortland, M. C., Hulley, C. B., Kagan, A., and Zukel, W. J. (1977) HDL cholesterol and other lipids in coronary heart disease. The cooperative lipoprotein phenotyping study, *Circulation 55*, 767−772.
2. Fielding C. J., and Fielding, P. E. (1981) Evidence for a lipoprotein carrier in human plasma catalyzing sterol efflux from cultured fibroblasts and its relationship to lecithin:cholesterol acyltransferase, *Proc. Natl. Acad. Sci. U.S.A. 78*, 3911−3914.
3. Fielding, C. J., Shore, V. G., and Fielding, P. E. (1972) A protein cofactor of lecithin:cholesterol acyltransferase, *Biochem. Biophys. Res. Commun. 46*, 1493−1498.
4. Acton, S., Rigotti, A., Landschulz, K. T., Xu, S., Hobbs, H. H., and Krieger, M. (1996) Identification of Scavenger Receptor SR-BI as a High Density Lipoprotein Receptor, *Science 271*, 518−520.
5. Brouillette, C. G., Anantharamaiah, G. M., Engler, J. A., and Borhani, D. W. (2001) Structural models of human apolipoprotein A-I: a critical analysis and review, *Biochim. Biophys. Acta 1531*, 4−46.
6. Frank, P. G., and Marcel, Y. L. (2000) Apolipoprotein A-I: structure−function relationships, *J. Lipid Res. 41*, 853−872.
7. Segrest, J. P., DeLoof, H., Dohlman, J. G., Brouillette, C. G., and Anantharamaiah, G. M. (1990) Amphipathic helix motif: classes and properties, *Proteins 8*, 103−117.
8. Segrest, J. P., Jackson, R. L., Morrisett, J. D., and Gotto, A. M., Jr. (1974) A Molecular Theory of Lipid−Protein Interactions in the Plasma Lipoproteins, *FEBS Lett. 38*, 247−253.
9. McLachlan, A. D. (1977) Repeated helical pattern in apolipoprotein A-I, *Nature 267*, 465−466.
10. Nolte, R. T., and Atkinson, D. (1992) Conformational analysis of apolipoprotein A-I and E−3 based on primary sequence and circular dichroism, *Biophys. J. 63*, 1221−1239.
11. Rogers, D. P., Roberts, L. M., Lebowitz, J., Datta, G., Anantharamaiah, G. M., Engler, J. A., and Brouillette, C. G. (1998) The Lipid-Free Structure of Apolipoprotein A-I: Effects of Amino-Terminal Deletions, *Biochemistry 37*, 11714−11725.
12. Meng, Q. H., Calabresi, L., Fruchart, J. C., and Marcel, Y. L. (1993) Apolipoprotein A-I domains involved in the activation of lecithin:cholesterol acyltransferase. Importance of the central domain, *J. Biol. Chem. 268*, 16966−16973.
13. Sorci-Thomas, M., Kearns, M. W., and Lee, J. P. (1993) Apolipoprotein A-I domains involved in lecithin-cholesterol acyltransferase activation. Structure:function relationships, *J. Biol. Chem. 268*, 21403−21409.
14. McManus, D. C., Scott, B. R., Frank, P. G., Franklin, V., Schultz, J. R., and Marcel, Y. L. (2000) Distinct Central Amphipathic α-Helices in Apolipoprotein A-I Contribute to the in vivo Maturation of High Density Lipoprotein by Either Activating Lecithin-Cholesterol Acyltransferase or Binding Lipids, *J. Biol. Chem. 275*, 5043−5051.
15. Laccotripe, M., Makrides, S. C., Jonas, A., and Zannis, V. I. (1997) The Carboxyl-terminal Hydrophobic Residues of Apolipoprotein A-I Affect its Rate of Phospholipid Binding and its Association with High Density Lipoprotein, *J. Biol. Chem. 279*, 17511−17522.
16. Huang, W., Sasaki, J., Matsunaga, A., Han, H., Li, W., Koga, T., Kugi, M., Ando, S., and Arakawa, K. (2000) A single Amino Acid Deletion in the Carboxyl Terminal of Apolipoprotein A-I Impairs Lipid Binding and Cellular Interaction, *Arterioscler., Thromb., Vasc. Biol. 20*, 210−216.
17. Brouillette, C. G., and Anantharamaiah, G. M. (1995) Structural models of human apolipoprotein A-I, *Biochim. Biophys. Acta 1256*, 103−129.
18. Gorshkova, I. N., Liu, T., Zannis, V. I., and Atkinson, D. (2002) Lipid-free structure and stability of apolipoprotein A-I: Probing the central region by mutation, *Biochemistry 41*, 10529−10539.
19. Borhani, D., Rogers, D. P., Engler, J. A., and Brouillette, C. G. (1997) Crystal structure of truncated human apolipoprotein A-I suggests a lipid-bound conformation, *Proc. Natl. Acad. Sci. U.S.A. 94*, 12291−12296.
20. Tricerri, M. A., Agree, A. K. B., Sanchez, S. A., and Jonas, A. (2000) Characterization of apolipoprotein A-I structure using a cysteine-specific fluorescence probe, *Biochemistry 39*, 14682−14691.
21. Agree, A. K. B., Tricerri, M. A., McGuire, K. A., Tian, S., and Jonas, A. (2002) Folding and stability of the C-terminal half of apolipoprotein A-I examined with a Cys-specific fluorescence probe, *Biochim. Biophys. Acta 1594*, 286−296.
22. Gorshkova, I. N., Liadaki, K., Gursky, O., Atkinson, D., and Zannis, V. I. (2000) Probing the lipid-free structure and stability of apolipoprotein A-I by mutation, *Biochemistry 39*, 15910−15919.
23. Mao, D., and Wallace, B. A. (1984) Differential light scattering and absorption flattening optical effects are minimal in the circular dichroism spectra of small unilamellar vesicles, *Biochemistry 23*, 2667−2673.
24. Pace, C. N., Shirley, B. A., and Thomas, J. A. (1989) in *Protein Structure* (Creighton, T. E., Ed.) pp 311−330, IRL Press, New York.
25. Gursky, O., and Atkinson, D. (1996) Thermal unfolding of human high-density apolipoprotein A-I: Implication for a lipid-free molten globular state, *Proc. Natl. Acad. Sci. U.S.A. 93*, 2991−2995.
26. John, D. M., and Weeks, K. M. (2000) Van't Hoff enthalpies without baselines, *Protein Sci. 9*, 1416−1419.
27. Atkinson, D., and Small, D. M. (1986) Recombinant Lipoproteins: Implications for Structure and Assembly of Native Lipoproteins, *Annu. Rev. Biophys. Biophys. Chem. 15*, 403−456.
28. Osborne, J. C., Jr., Lee, N. S., and Powell, G. M. (1986) Solution properties of apolipoproteins, *Methods Enzymol. 128*, 375−387.
29. Rogers, D. P., Roberts, L. M., Lebowitz, J., Engler, J. A., and Brouillette, C. G. (1998) Structural Analysis of Apolipoprotein A-I: Effects of Amino- and Carboxy-Terminal Deletions on the Lipid-Free Structure, *Biochemistry 37*, 945−955.
30. Reynolds, J. A. (1976) Conformational stability of the polypeptide components of human high-density serum lipoprotein, *J. Biol. Chem. 251*, 6013−6015.
31. Barbeau, D. L., Jonas, A., Teng, T., and Scanu, A. M. (1979) Asymmetry of apolipoprotein A-I in solution as assessed from ultracentrifugal, viscometric, and fluorescence polarization studies, *Biochemistry 18*, 362−369.
32. Strickland, E. H. (1974) *CRC Crit. Rev. Biochem. 2*, 113−175.
33. Woody, R. W., and Dunker, A. K. (1996) Aromatic and cysteine circular dichroism in proteins, in *Circular Dichroism and the Conformational Analysis of Biomolecules* (Fasman, G. D., Ed.) pp 109−158, Plenum Press, New York and London.
34. Davidson, W. S., Hazlett, T., Mantulin, W. W., and Jonas, A. (1996) The role of apolipoprotein A-I domains in lipid binding, *Proc. Natl. Acad. Sci. U.S.A. 93*, 13605−13610.
35. Rogers, D. P., Brouillette, C. G., Engler, J. A., Tendian, S. W., Roberts, L., Mishra, V. K., Anantharamaiah, G. M., Lund-Katz, S., Phillips, M. C., and Ray, M. J. (1997) Truncation of the amino terminus of human apolipoprotein A-I substantially alters only the lipid-free conformation, *Biochemistry 36*, 288−300.
36. Langner, M., Cafiso, D., Marcelio, S., and McLaughlin, S. (1990) Electrostatics of phosphoinositide bilayer membranes. Theoretical and experimental results, *Biophys. J. 57*, 335−349.
37. Scholtz, J. M., Marqusee, S., Baldwin, R. L., York, E. J., Stewart, J. M., Santoro, M., and Bolen, D. W. (1991) Calorimetric determination of the enthalpy change for the α-helix to coil transition of an alanine peptide in water, *Proc. Natl. Acad. Sci. U.S.A. 88*, 2854−2858.
38. Lu, B., Morrow, J. A., and Weisgraber, K. H. (2000) Conformational reorganization of the four-helix bundle of human apolipoprotein E in binding to phospholipid, *J. Biol. Chem. 275*, 20775−20781.
39. Gursky, O. (2001) Solution conformation of human apolipoprotein C-1 inferred from proline mutagenesis: Far- and Near-UV CD study, *Biochemistry 40*, 12178−12185.
40. Narayanaswami, V., Wang, J., Schieve, D., Kay, C. M., and Ryan, R. O. (1999) A molecular trigger of lipid binding-induced opening of a helix bundle exchangeable apolipoprotein, *Proc. Natl. Acad. Sci. U.S.A. 96*, 4366−4371.

BI034152T